Sciences & Technologie **A – N°20**, Décembre (2003), pp. 83-88.

MONTE CARLO SIMULATION OF CHARGED PARTICLE IN AN ELECTRONEGATIVE PLASMA

Received 30/06/2002 – Accepted 02/03/2003

Abstract

Interest in radio frequency (rf) discharges has grown tremendously in recent years due to their importance in microelectronic technologies. Especially interesting are the properties of discharges in electronegative gases which are most frequently used for technological applications. Monte Carlo simulation have become increasingly important as a simulation tool particularly in the area of plasma physics. In this work, we present some detailed properties of rf plasmas obtained by Monte Carlo simulation code, in SF_6.

***Keywords**: Monte Carlo simulation; glow discharge; radio frequency; plasma.*

Résumé

L'intérêt pour les décharges radio fréquence (rf) s'est considérablement accru ces dernières années, vu leur importance dans les technologies microélectroniques. Un intérêt particulier est attribué aux propriétés des décharges dans des gaz électronégatifs, fréquemment utilisés dans des applications technologiques. La méthode de Monte Carlo a pris une importance croissante en tant qu'outil de simulation, et plus particulièrement dans le domaine de la physique des plasmas. Dans ce travail, nous présentons certaines propriétés des plasmas rf obtenus par le code de simulation de Monte Carlo, et ce, pour le SF_6.

***Mots clés**: Simulation de Monte Carlo; Décharge électrique; radio fréquence; plasma.*

L. SETTAOUTI
A. SETTAOUTI
M. SEBBANI
Département d'Electrotechnique
Université d'Oran (USTO)
BP.1505 Oran El-M'naouar
Oran, Algérie

ملخص

إن الاهتمام بالتفريغ تردد الراديو أزداد كثيرا في الأعوام الأخيرة وذلك لأهميته في تقنيات الإلكترونيات الصغيرة الدقيقة وخاصة الاهتمام بخصوصية التفريغ في غاز سالب التكهرب الذي يكثر استعماله في التطبيقات التكنولوجية. في هذا البحث نقدم بعض الخصوصيات المفصلة للبلازما تردد الراديو الموجودة عن طريق محاكاة مونت كار لو في غاز سالب التكهرب.

***الكلمات المفتاحية:** محاكاة مونت كارلو، التفريغ الكهربائي، تردد الراديو، البلازما.*

Weakly ionized plasmas generated by RF glow discharges have become increasingly used and studied for many applications, such as plasma etching, and thin film deposition for the microelectronic industry [1-3]. Consequently, there has been significant interest in developing models for these plasma based processes. A validated process model has several benefits ranging from providing an understanding of mechanisms and in process control to aid in equipment design. Process models for dry etching and plasma deposition are complex since weakly ionized discharges used in materials processing are characterized by complex interactions between discharge physics, chemistry and surface processes. Since it is difficult to decouple any of these interactions in practice, tractable models can only be developed through judicious approximations guided by intuition, experience gained from similar fields and by validation against experiments.

To better understand the RF discharge of etching gases and etching mechanism, it is important to know the kinds of radical and ion species present in the plasma. RF discharge plasmas in electronegative gases have been widely used in the microelectronics industry. In such plasmas, negative ions affect the discharge characteristics as follows. the electrical conductivities of the discharge plasmas decrease because a large number of electrons attach to neutrals and form many massive negative ions. RF discharge plasmas in SF_6 (sulfur hexafluoride) and SF_6 mixture gases have been widely utilised in plasma processing. And the studies of SF_6 have been motivated by the importance of this gas for plasma etching of metals and silicon, for negative ion sources, and in development of gaseous dielectrics [4-11]. In the past statistically designed experiments have been used, together with simple reaction diffusion, and electrical analog models to design industrial processes, and to study the phenomena within the plasma. All these efforts try to shed light a posteriori to the plasma dynamics are available, similar to the ones used for solid state devices.

The lack of such tools for simulation of the plasma dynamics is partly due to the synergy of the many phenomena that simultaneously take place and complicate the plasma process. Plasma process modelling can be broken into modules which describe the plasma physics, the transport of gaseous species and the gas and surface chemistry. At a later stage the modules can be merged by including the interactions among them. A current challenge in designing plasma processing tools is the development of computer models of rf discharges that can accurately describe non-equilibrium charged particle transport and plasma chemistry, yet execute quickly enough to make more realistic multidimensional simulations feasible. The goal is then to make discharge modeling an integral part of the discharge reactor design process [12,13].

As plasma processes become increasingly important, there is a renewed interest to understand the plasma dynamics, i.e., the interaction of charged particles in the plasma with the electric fields and the physical phenomena that this interaction induces. Fluctuations in RF plasmas make experimental investigation of their properties in space and time difficult. The motivation for the development of the computer simulation described in this paper has its basis in the need to quantitatively understand microelectronic plasma processing. The following section is devoted to the method of simulation.

METHOD OF SIMULATION

The Monte Carlo methods as applied to gas discharge problems involve evaluating the percentage of a given species of particles emanating from a given source, after experiencing energy loss and gain, terminate in defined categories. The computing time for the Monte Carlo technique depends upon the number of test electrons released from the space of the interval and the number of collisions occurring while each electron travels the distance from the cathode to the anode.

Glow discharges rf at 13.56 MHz are being used in many fields of application. A wide range of parameter space can be chosen to operate the plasma processes. The electron transport in a gas under the influence of an electric field E can be simulated with the help of a Monte Carlo method. [2,12-15] Every electron, during its transit in the gas, performs a succession of free flights punctuated by elastic or inelastic collisions with molecules of gas defined by collision cross sections. During the successive collisions for every electron, certain information (velocity, position, etc.) is stored in order to calculate, from appropriate sampling methods, transport coefficients and macroscopic coefficients.

Electron trajectories are computed using Monte Carlo method for an rf parallel plate discharge in a molecular gas (pure SF_6) while oscillating the applied electric field providing a time and spatially dependent electric field, many rf cycles are computed. A simple group of electrons, typically 300-500, is randomly seeded between the electrode plates with a Maxwellian distribution having a temperature of 5 eV (The electric field in the first cycle oscillates with a period corresponding to the rf cycle, and the plasma is not established). The applied electric field is oscillated at rf frequencies providing a time and spatially dependent electric field, and electron trajectories are calculated using the Monte Carlo method. The three dimensional motion of electrons between two successive collisions under the electric field is solved numerically with use of Euler method. Electron flight time between two successive collisions is determined by the electron collision cross section with a SF_6 molecular gas.

The electrode system is assumed to consist of parallel plates with a diameter that is larger than the electrode separation. Interactions with the electrodes are not considered. The secondary electron emission coefficient due to electrons flowing to the two electrodes is assumed to be zero. The electron undergoes many ionizing collisions in each of which an ion and another electron are formed. Thus, we obtain an expanding cloud of electrons traveling toward the anode, known as electron avalanche, and a cloud of ions, almost stationary in the time scale of motion of the electron avalanche, remaining behind.

The probability of collision and the nature of collision are simulated by comparison with computer generated random numbers.

The probability of collision in the time step ΔT is

$$P = 1 - \exp\left(\frac{-\Delta T}{T_m}\right) \quad (1)$$

T_m is the mean collision time.

At t = 0, an electron observes a free flight time with a randomly selected angle of entry depending on the distribution. And the collision is simulated by comparing P with R_1 at the and of each step. where R_1 is a random number uniformly distributed between 0 and 1. When the electron undergoes a collision

$$P = \left[1 - \exp\left(\frac{-\Delta T}{T_m}\right)\right] \geq R_1 \quad (2)$$

The type of collision is determined according to figure 1, where the position of the arrow indicates the nature of collision Q_i / Q_T gives the probability of the coming process. Hence, after the event of a collision if the probabilities of inelastic collisions fail the collision is deemed to be elastic and the loss of energy in the collision is 2m / M where m and M are the masses of electron and a SF_6 molecule, respectively.

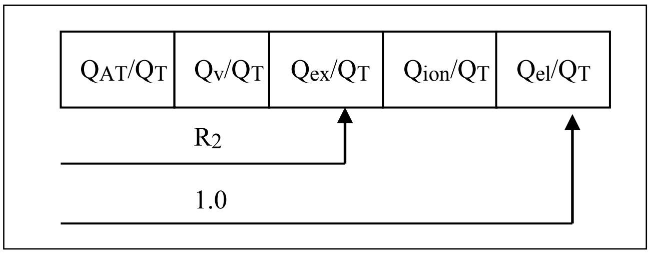

Figure 1: Scheme for deciding on the nature of collision.

And R_2 is again a random number uniformly distributed between 0 and 1. The total collision cross section is defined as

$$Q_T = Q_{el} + Q_{At} + Q_v + Q_{ex} + Q_{ion}$$

where Q_{el} is the elastic cross section which is replaced by the momentum transfer collision cross section in the simulation; Q_{At} is the attachment cross section, Q_{ex} the total electronic excitation cross section, Q_v the vibrational cross section, and Q_{ion} is the total ionization cross section.

The scattering after all collisions is assumed to be isotropic. The assumption of isotropic scattering is a hypothesis which is consistent with the first order theory if, at the same time the total collision cross section is replaced by the momentum transfer cross section. The distribution of the electric field E(x,t) is calculated from the following solution of the one dimensional Poisson's equation with the use of the electron and ion densities at the end of each time step. The total number of electrons in the gap increases over many orders of magnitude, hence scaling is necessary to limit the number of simulation particles. When, the total number of simulation particles, exceeds the maximum allowable number of simulation particles, which is specified in the program input data, a statistical subroutine is introduced to choose a new group of larger particles to represent the old larger group of smaller particles. The subroutine contains a weighing of velocity distribution of the old group, so that the new group is equivalent in phase space to the old group.

RESULTS AND DISCUSSION

In this paper we present typical results of numerical simulations using a Monte Carlo method of rf plasmas sustained by an rf external source of 13.56 MHz and 200 V, in an Sulfur hexafluoride model gas (pure SF_6). Electrode separation and gas pressure used are 2 cm and 0.6 Torr, respectively.

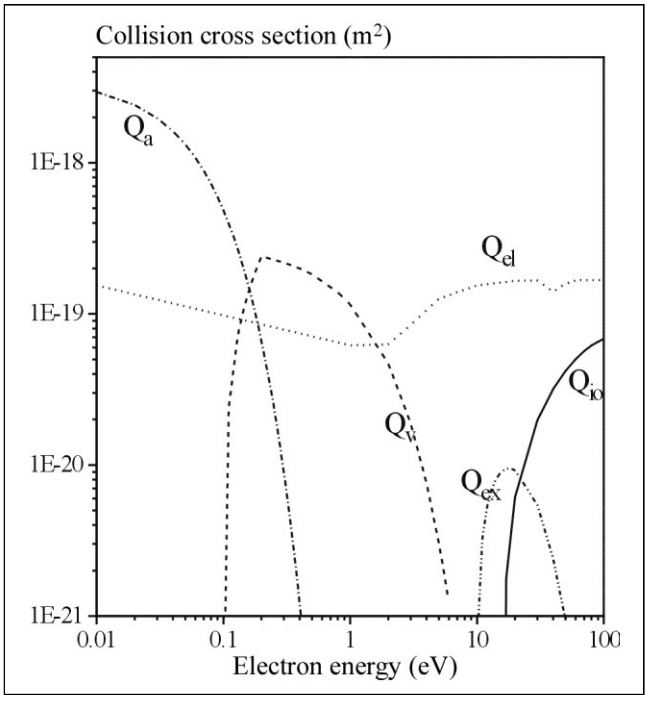

Figure 2: Summary of collisional cross section of SF_6: Q_{el}: elastic momentum transfer cross section; Q_{At}: attachment, Q_{ex}: electronic excitation, Q_v: vibrations, and Q_{ion}: ionization .

The cross section set of SF_6 employed (Fig. 2) is that of Hayes *et al*, [16] Peach [17,18] and Itoh *et al*. [19].

It is seen from figure 3.1 the electric field in the first cycle oscillates with a period corresponding to the rf cycle. And in the figure 3.2 shows that the mean electron energy in the first rf cycle is maximum when the electric field for this cycle is maximum, and minimum where the electric field is minimum. And is almost spatially constant, and oscillates with the rf external field.

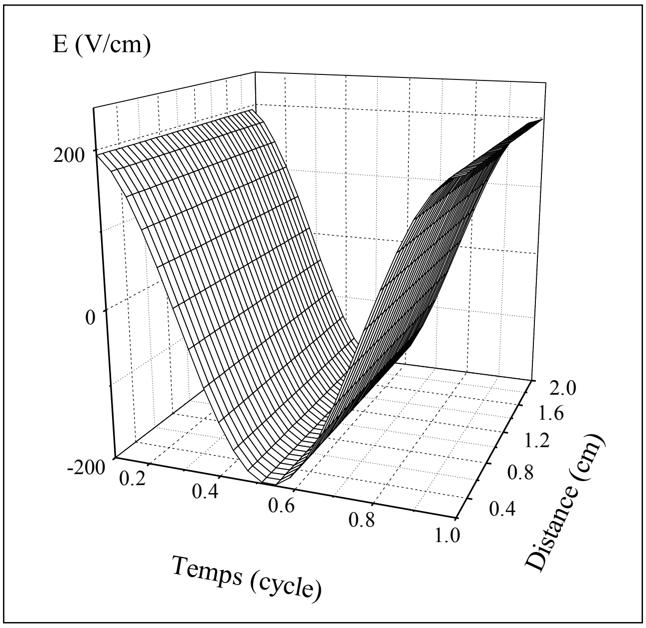

Figure 3.1: Temporal and spatial variations of the electric field for the first cycle.

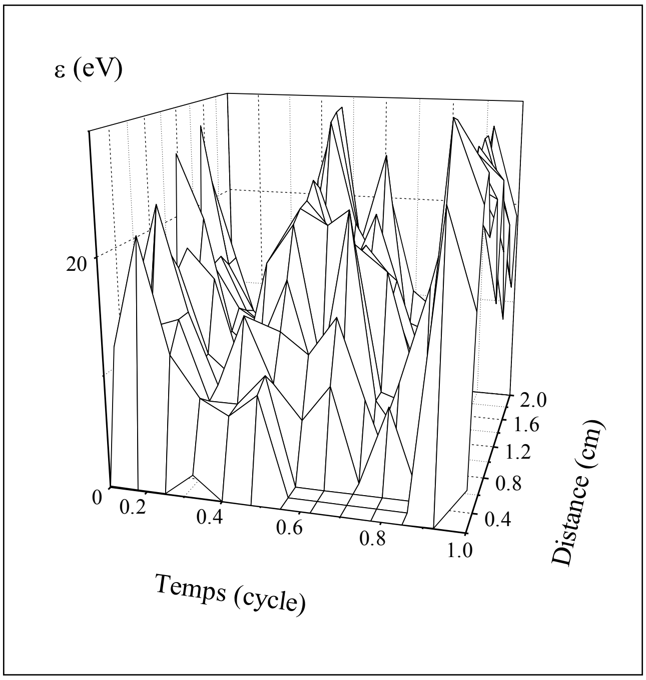

Figure 3.2: Temporal and spatial variations of the mean energy of electrons for the first rf cycle.

It is seen from figure 3.3 the electron density is low at the beginning of the avalanche growth, as time increases, the enhancement becomes greater. And oscillate with the change in the direction of the electric field.

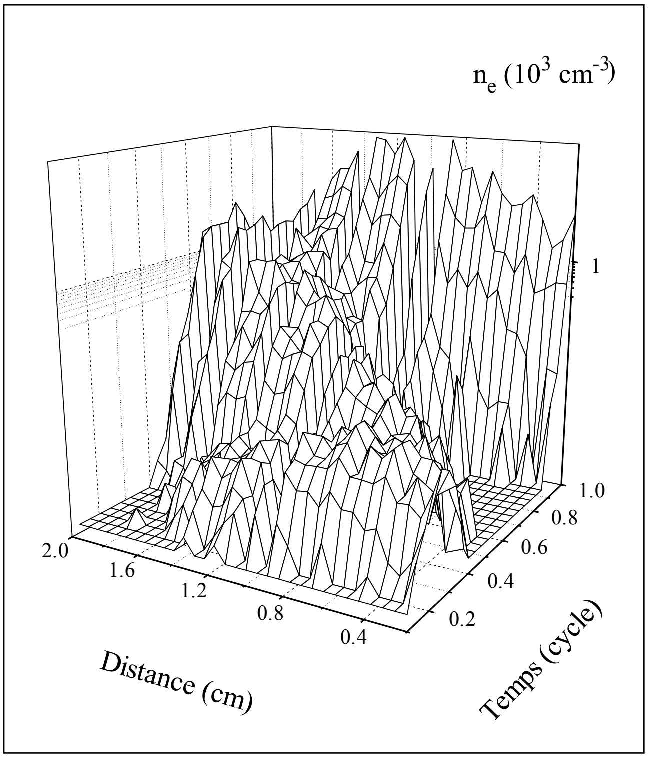

Figure 3.3: Temporal and spatial variations of the electron density for the first rf cycle.

Figure 4.1 shows, the spatial and temporal evolution of the electric field during the second rf cycle. The space charge field distortion begins, The field behind and ahead of the avalanche is enhanced, while in the bulk of the avalanche it is weakened by space charge field. In an electronegative gas, because of attachment, the electron number is less than of the positive ion, and enhances the field behind the avalanche.

And in the figure 4.2 shows, the spatial and temporal evolution of the electric field during the third rf cycle, when the plasma is established (half cycle).

The electric fields in the bulk are small and most of the voltage difference is concentrated in the sheaths. The electric field profile as a function of time and space is shown in figure 4.2. In the center and close to the electrodes the temporal modulation of electric fields is fairly well represented by a sinusoid with little dc bias.

The sheath effects (characterized by a rapid decrease of electric field) can be clearly observed in the vicinity of the electrodes. There are two distinct regions with respect to the flow of electron energy in a parallel plate rf discharge, the bulk plasma and the sheaths.

The electric field for the discharge is symmetric about the discharge mid-plane (The simulation results show that there are two distinct regions, the bulk plasma and the sheaths).

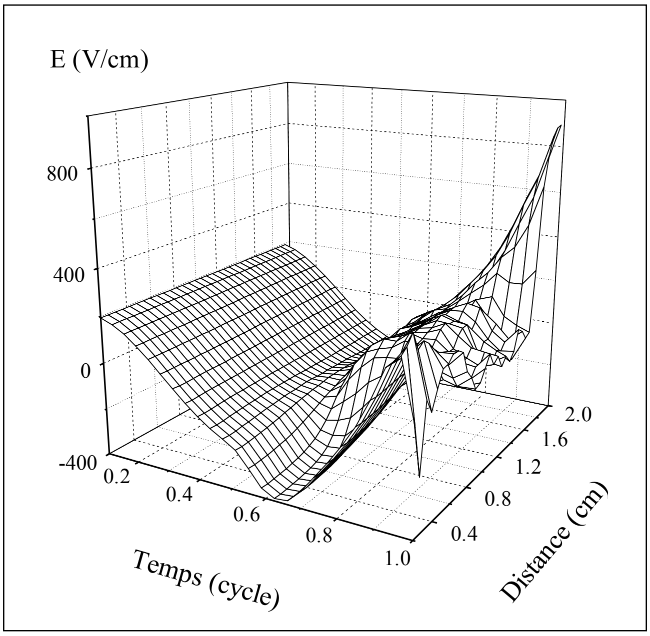

Figure 4.1: Temporal and spatial variations of the electric field for the second cycle.

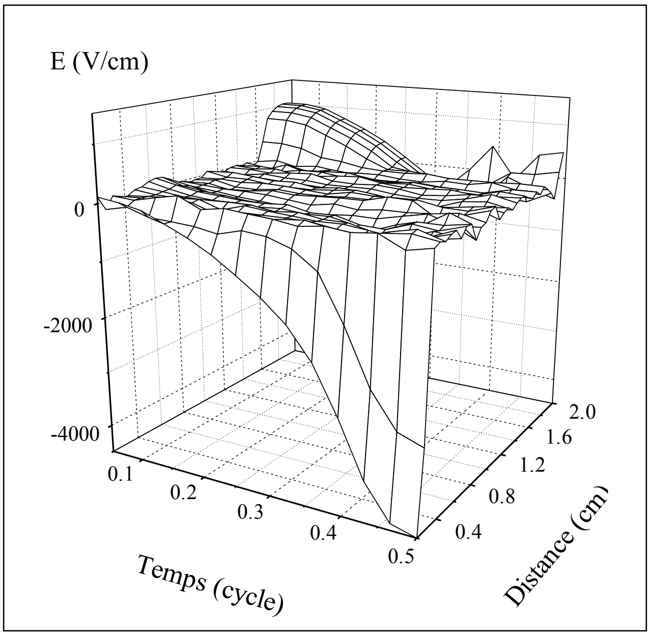

Figure 4.2: Temporal and spatial variations of the electric field for the third cycle.

As the cycle advances, electrons are pushed out of the right sheath and into the left one. The movement of electrons causes a modulation of sheath width (the apparent sheath thickness is 0.3 cm). The sheaths are quite wide causing the discharge to behave capacitively. Electrons are contained in the plasma in part by the space charge fields developed from the difference of positive and negative ion concentration near the wall. Depending on the phase of the applied potential, electrons move toward either electrode. Their movement affects the local fields causing electrons to pile in the bulk sheath interface. Thus, peak appear in the electron density, which is shown in figure 5.1 as a function of position and time. The large electric fields contribute to the formation of the peaks in the electron density.

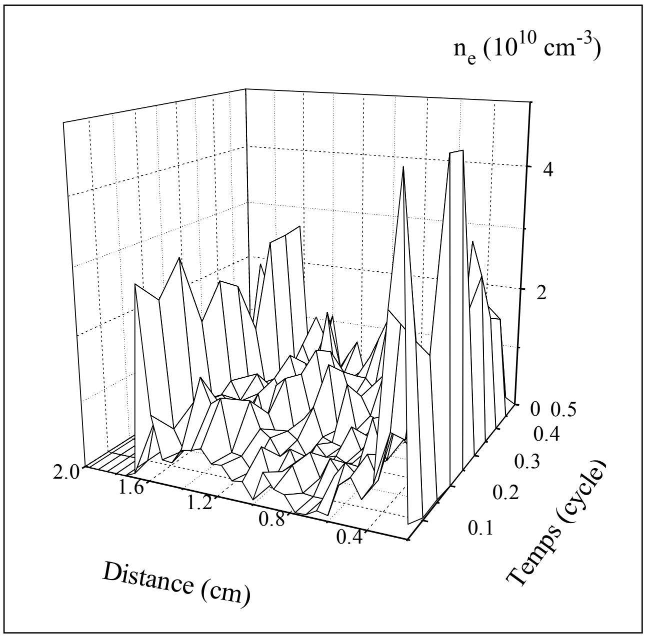

Figure 5.1: Temporal and spatial variations of the electron density for the third rf cycle.

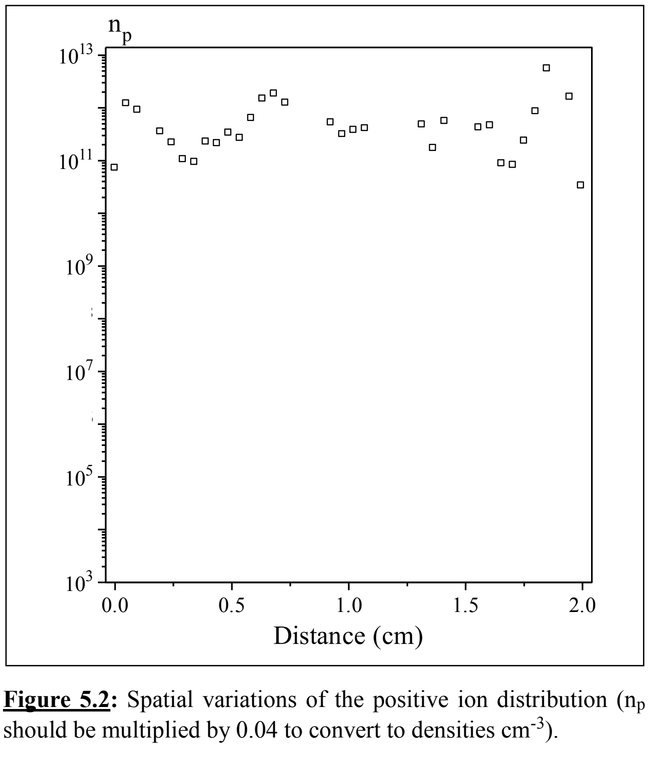

Figure 5.2: Spatial variations of the positive ion distribution (n_p should be multiplied by 0.04 to convert to densities cm^{-3}).

Ion densities are not modulated significantly in time.

The Positive ions (SF_6^-) due to the ionization and the negative ions (SF_6^+) due to the attachment of the electronegative gas (Fig. 5.2. and 5.3) have approximately the same densities in the bulk of the plasma, and they differ only in the very thin sheath near the electrodes.

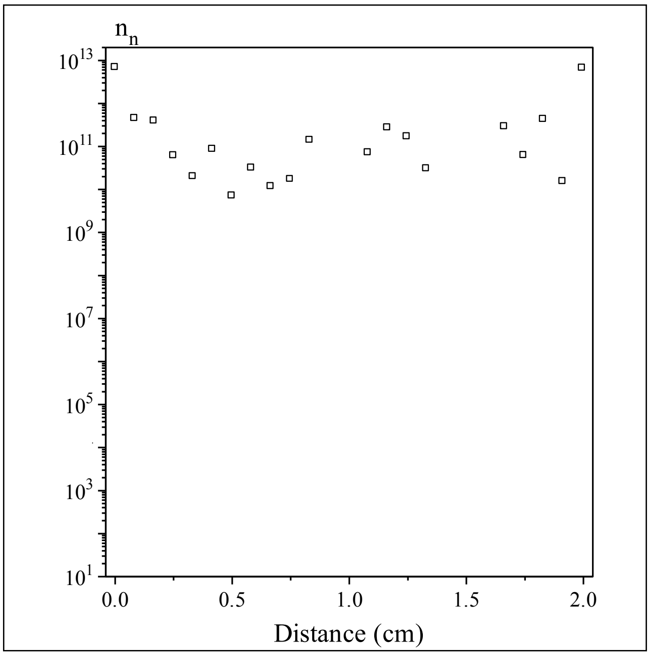

Figure 5.3: Spatial variations of the negative ion distribution (n_n should be multiplied by 0.04 to convert to densities cm^{-3}).

In figure 6, the spatiotemporal profiles of the electron mean energy show the different natures of the three regions in the discharge. The electron mean energy is nearly constant and uniform through the plasma bulk region and the relatively large modulations take place in sheath regions. The discharge parameters are symmetric about the discharge mid-plane.

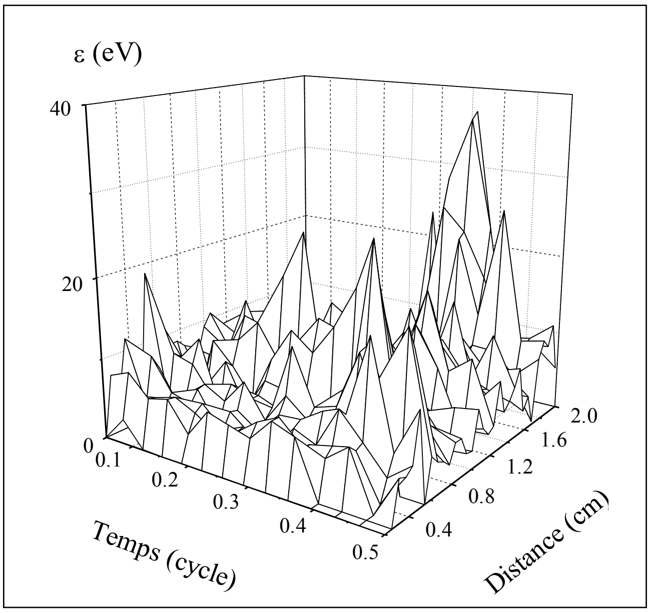

Figure 6: Temporal and spatial variations of the mean energy of electrons for the third rf cycle.

Such a maximum in the electric field in the sheath regions create a maximum in the average electron energy shown in figure 6. (here the secondary electron emission was assumed to be zero). Indeed the maximum in the electric field are close to the maximum in energy, but not exactly at the same position in space or time because we do not assume local equilibrium with the field. And is almost constant in time and space in the bulk region, when the electric field is minimum.

The calculated electric field and sheath thickness compared with the measured values [20,21], the agreement between our results and those referred to above is very good.

CONCLUSION

We have developed a numerical code for Monte Carlo simulation of rf plasmas in an electronegative (SF_6) model gas. We have investigated how many rf cycles have to be followed with the Monte Carlo model before the establishment of the plasma.

The simulation results show that there are two distinct regions with respect to the flow of electron energy in a parallel plate rf discharge, the bulk plasma and the sheaths. The electric field is maximum in the sheath and minimum in the bulk region. The electric field in the sheath changes almost linearly from both electrodes to the edge region of the bulk plasma. Most of rf external electric field is absorbed in the sheath regions. The movement of electrons causes a modulation of sheath width. The sheaths are quite wide causing the discharge to behave capacitively.

The positive and negative ions have approximately the same densities in the bulk of the plasma. And the electron density have two peaks in the bulk sheath interface.

REFERENCES

[1]- S.W. Choi, G. Lucovsky and K.J. Bachmann, "Remote Plasma Enhanced Chemical Vapor Deposition of GaP with in situ Generation of Phosphine Precursors", *J. Vac. Sci. Technol.*, B10(3), (1992), pp. 1070-1073.

[2]- S.S. Nathan, G.M. Rao, S. Mohan, "Transport of Sputtered Atoms in Facing Targets Sputtering Geometry: A Numerical Simulation Study", *J. Appl. Phys*., 84(1), (1998), pp. 564-571.

[3]- De-Zhen Wang, J.Q. Dong, "Kinetics of low pressure rf discharges with dust particles", *J. Appl. Phys*., 81(9), (1997), pp. 38-42.

[4]- Z. Lj. Petrovic, F. Tochikubo, S. Kakuta, T. Makabe, "Spatiotemporal Optical Emission Spectroscopy of rf discharges in SF_6", *J. appl. Phys.*, 73(5), (1993), pp. 2163-2172.

[5]- H.C. Sun, E.A. Whittaker, "Real-Time in situ Detection of SF_6 in a Plasma Reactor", *Appl. Phys. Lett*., 63(8), (1993), pp. 1035-1037.

[6]- S.B. Radovanov, B. Tomcik, Z. Lj. Petrovic, B.M. Jelenkovic, "Optical Emission Spectroscopy of rf Discharge in SF6", *J. appl. Phys*., 67(1), (1990), pp. 97-107.

[7]- S.J. Kim, K. Shin, H.K. Park, "Dry Post-Etch Treatment Using SF6 Chemistry for 0.2 μm Contact Hole", *Jpn. J. Appl. Phys.*, 34(3A), (1995), pp. 5001-5005.

[8]- K. Nagaseki, I. Ishikawa, E. Nishimura, Y. Saito, S. Suganomata, "Negative Ions in 13.56 MHz discharge of SF6 gas in a Planar Diode", *Jpn. J. Appl. Phys*., Vol. 34, (1995), pp. L852-L855.

[9]- K. Nagaseki, H. Kobayashi, I. Ishikawa, E. Nishimura, Y. Saito, S. Suganomata, "Mass Spectrometry of Discharge Products at 13.56 MHz in SF6 Gas", *Jpn. J. Appl. Phys*., 33(7B), (1994), pp. 4348-4352.

[10]- H. Nakayama, M. Onoda, T. Nishida, T. Kubota, H. Kamatani, K. Watabe, "Creeping Discharge Characteristics under Rectangular Pulse Voltage in SF6 Gas", *Jpn. J. Appl. Phys*., 35(7), (1996), pp. 4079-7080.

[11]- D.M. Xiao, X.G. Li, X. Xu, "Swarm Parameters in SF6 and CO2 Gas Mixtures", *J. Phys. D: Appl. Phys*., 34, (2001), pp. L133-L135.

[12]- M.J. Grapperhaus, M.J. Kushner, "A Semianalytic Radio Frequency Sheath Model Integrated into a two dimensional Hybrid Model for Plasma Processing Reactors", *J. Appl. Phys.*, 81(2), (1997), pp. 569-577.

[13]- W. Helin, L. Zuli, L. Daming, "Monte Carlo Simulation for Electron Neutral Collision Processes in Normal and Abnormal Discharge Cathode Sheath Region", *Vacuum*, 47(9), (1996), pp. 1065-1072.

[14]- A. Settaouti, A. Mimouni, "Monte Carlo Simulation of Electron Swarms in SF6 in Uniform Electric Fields", The Third International Conference on Computational Aspects and Their Applications in Electrical Engineering, "CATAEE'99", Philadelphia University, Jordan, 19-20 Oct. (1999), pp. 123-128.

[15]- A. Settaouti, L. Aouabdi, "Monte Carlo Simulation of Electron Swarms in Nitrogen in Uniform Electric Field", 4th Jordanian International Electric & Electronics Engineering Conference 2001 (JIEEEC'2001), Amman-Jordan, 16-18 April (2001), pp. 265-269.

[16]- T.R. Hayes, R.C. Wetzel and R.S. Freund, "Absolute Electron -impact-ionization Cross Section Measurement of the Halogen Atoms", *Phys. Rev*., 35(2), (1987), pp. 578-584.

[17]- G. Peach, "Ionization of Neutral Atoms with Outer 2P, 3S, and 3P Electrons by Electron and Proton Impact", *J. Phys. B: Atomic Molec. Phys*., Vol. 3, (1970), pp. 328-349.

[18]- G. Peach, "Ionization of Atoms and Positive Ions by Electron and Proton Impact", *J. Phys. B: Atomic Molec. Phys*., Vol. 4, (1971), pp. 1670-1677.

[19]- H. Itoh, Y. Miura, N. Ikuta, Y. Nakao and H. Tagashira, "Electron Swarm Development in SF6 I: Boltzmann Equation Analysis", J. *Phys. D: Appl. Phys*., Vol. 21, (1988), pp. 922-930.

[20]- A.H. Sato, M.A. Lieberman, "Electron-Beam Probe Measurement of Electric Fields in rf Discharges", *J. Appl. Phys*., 68 (12), (1990), pp. 6117-6124.

[21]- F. Becker, I.W. Rangelow, R. Kassing, "Ion Energy Distributions in SF_6 Plasmas at a Radio-Frequency Powered Electrode", *J. Appl. Phys*., 80 (1), (1996), pp. 56-65. □